Transient investigation of mini-channel regenerative heat exchangers:

Alfarawi, Suliman; Al-Dadah, Raya; Mahmoud, Saad

DOI:
10.1016/j.applthermaleng.2017.07.038

Document Version
Peer reviewed version

Citation for published version (Harvard):
Alfarawi, S, Al-Dadah, R & Mahmoud, S 2017, 'Transient investigation of mini-channel regenerative heat exchangers: Combined experimental and CFD approach', *Applied Thermal Engineering*, vol. 125, pp. 346-358. https://doi.org/10.1016/j.applthermaleng.2017.07.038

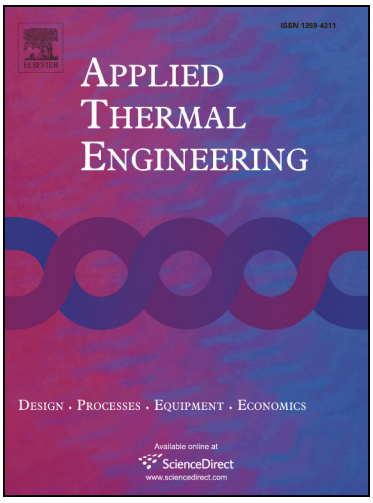

Research Paper

Transient investigation of mini-channel regenerative heat exchangers: Combined experimental and CFD approach

S. Alfarawi, R. AL-Dadah, S. Mahmoud

PII: S1359-4311(17)32013-6
DOI: http://dx.doi.org/10.1016/j.applthermaleng.2017.07.038
Reference: ATE 10705

To appear in: *Applied Thermal Engineering*

Received Date: 25 March 2017
Revised Date: 28 June 2017
Accepted Date: 3 July 2017

Please cite this article as: S. Alfarawi, R. AL-Dadah, S. Mahmoud, Transient investigation of mini-channel regenerative heat exchangers: Combined experimental and CFD approach, *Applied Thermal Engineering* (2017), doi: http://dx.doi.org/10.1016/j.applthermaleng.2017.07.038

Transient investigation of mini-channel regenerative heat exchangers: Combined experimental and CFD approach

S. Alfarawi[1,a], R. AL-Dadah[1], S. Mahmoud[1]

[1]*Department of Mechanical Engineering, University of Birmingham, Edgbaston, B15 2TT, UK*

[a]e-mail: ssa178@bham.ac.uk

Abstract

This paper presents a combined approach based on experiment and CFD as an alternative to single-blow method to investigate heat transfer and flow friction of three mini-channel regenerative heat exchangers (MCRHX), having channel hydraulic diameters of 1.5, 1 and 0.5mm. Experiments were conducted to measure pressure drop and the transient thermal responses at the inlet and outlet of each MCRHX. The thermal response predicted from CFD, based on transient conjugated heat transfer simulations, was iteratively solved until it matched the experimental data within an acceptable deviation. The results showed that 0.5mm MCRHX had the highest interstitial heat transfer coefficient due to the increased specific surface area. However, the penalty is the increased pressure drop. Moreover, Nusselt number and friction factor correlations were obtained for each configuration to correlate mini-channel heat transfer characteristics.

Keywords: Heat transfer, pressure drop, Transient testing, CFD, Experiment, mini-channel.

Nomenclature

C_p	Heat capacity at constant pressure, J/kg· K	h	Hydraulic
D	Diameter, m	i	Inner, inlet
h	Heat transfer coefficient, W/m^2. K	o	Outer, outlet
k	Thermal conductivity, W/m. K	ref	Reference value
L	Heat exchanger length, m	s	Solid
P	Pressure, Pa	W	Wall
q_sf	Interstitial heat transfer coefficient, W/m^3. K	***Dimensionless Terms***	
q″	Net heat flux, W/m^2	f	Darcy friction factor
t	Time, s	j	Colburn factor
T	Temperature, K	Nu	Nusselt number
U_m	Flow mean velocity, m/s	Pr	Prandtl number
Greek letters		Re	Reynolds number
Δ	Difference	Θ	Temperature incremental rate
ν	Air kinematic viscosity, m^2/s	τ	Time scale
μ	Air dynamic viscosity, Pa. s	ε	Volumetric porosity
ρ	Air density, kg/m^3	ζ	Overweighing constant
Subscripts		***Abbreviations***	
b	Bulk	CFD	Computational fluid dynamics
cal	Calculated	SCFM	Standard cubic feet per minute
exp	Experimental	MCRHX	Mini-channel regenerative heat exchanger
f	Final value		

1- Introduction

The proper utilization of energy resources can lead to a successful development of an efficient and cost effective heat exchangers. A heat exchanger is a device that transfers thermal energy between a solid object and a fluid or between two or more fluids. Various types of heat exchangers are widely used in industry and production lines. An accurate evaluation of heat transfer coefficient between fluid and solid interfaces in heat exchangers is required when fluid flow is so ill-defined. Based on the channel hydraulic diameter, heat exchangers can be classified into; conventional channels ($D_h > 3mm$), mini-channels ($3mm \geq D_h > 200\mu m$) and micro-channels ($200\mu m \leq D_h \leq 10\mu m$) [1]. It is difficult to measure heat transfer coefficients in micro /mini channels heat exchangers due to small pore size and the unavailability of such tiny probes to measure the channels surface temperature. The thermal performance of heat exchangers and thermal regenerators are commonly evaluated by single-blow technique. This transient technique is cost-effective and less time consuming compared to steady state method. The methodology is simple and it is composed of three steps; an experiment, theoretical model and a matching technique. In the test facility, the sample (heat exchanger) undergoes a step change in temperature at the inlet, depending on fluid type and matrix heat capacity, the outlet temperature breakthrough is sampled to be compared with any appropriate theoretical model. Hausen [2] originally formulated the mathematical model for transient method. Schumann [3] solved analytically the transient problem. Locke [4] showed that a unique relationship exists between the maximum slopes of the outlet response curves and the number of heat transfer units (NTU) for a step change for the fluid at the inlet of the heat exchanger but the effect of axial conduction was not accounted. The Schumann-Hausen model was found unrealistic based on the assumptions made. Loehrke [5] showed that it is not practical to conduct an experiment with an ideal temperature step change. The knowledge of the mathematical formulation of the inlet temperature curve, it became possible to use an arbitrary fluid temperature. Exponential fluid inlet variation was reported by Liang and Yang [6], Cai et al. [7] and Mullisen and Loehrke [8]. Moreover, the core matrix or heat exchanger is in contact with walls and in many applications, the adiabatic wall is a poor assumption. In other words, the outlet fluid temperature is influenced by the heat losses dissipated to the walls in the test section. Chen and Chang [9] showed that in their experiment that the NTU values were underestimated by 30% due to the adiabatic wall assumption. In addition, the Joule-Thomson effect is more common when the flow encountered a restriction causing the fluid temperature to rise or drop. Chen et al. [10] showed that considering this effect for a wire regenerator (No 200), the drop in outlet temperature was 3% when higher pressure drop was achieved at 0.2 MPa. Other researchers have improved the Schumann-Hausen model to correctly match the experiments of

single-blow method. Pucci et al. [11] included the effect of axial conduction and improved Locke's analysis. They showed that this effect is dominant when the NTU value >2. It followed that some researchers included radial conduction effect due to the non-uniformity of flow [12]. Heggs and Burns [13] showed that neglecting longitudinal or transverse conduction or idealizing the temperature input function as an ideal step may cause inaccurate estimation of heat transfer processes. A comprehensive review on transient techniques are provided in [14]. Different evaluation techniques have been developed to compare the predicted and measured fluid exit temperature histories; maximum slope method [4], Selected point matching technique [7], Differential fluid enthalpy method (DFEM) [15] and Direct curve matching [13]. Mismatching between the experiment and the model can be potential and far from correct even if two methods give similar results. Loehrke [5] recommended pre-calibration of the test facility with a well-known core performance. However, more recently, both the maximum gradient technique and curve matching at multiple points are used [10, 12, 16-18]. Optimization of heat emission and pressure drop of mini-channel by regulating the channel size and length has been recently investigated by [19]. Extensive reviews were conducted on micro/minichannels in terms of heat transfer and pressure drop characteristics of single and two-phase flow [20-21]. They showed that pressure drop from exprimental data in little agreement with prediction. In terms of thermal behavior, the agreement is becoming closer when the hydrulic diameter increases for single phase flow. In small scale of microchannels ($1\mu m$), the rarefied gas effects come into play [22]. Three regimes of flow are encountered depending on Knudsen number (mean free path/characteristic length); continuum flow, slip flow and free-molecular flow. Mini-channel heat transfer is an active area of research due to its light weight, compactness and high heat transfer rate. Caney *et al* [23] conducted an experimental study on friction losses and heat transfer of single-phase flow in a mini-channel. They showed that the experimental frictional pressure drop measurements agree accurately with the conventional correlations while the temperature profile along the channel length deviates from the linear trend due to axial wall conduction. Liu and Yu [24] showed that mini-channel heat sink performance can be enhanced by using non uniform baffles at the inlet of channels which provide more unformity of the temperature. On the other hand, Khoshvaght-Aliabadi *et al* [25] proposed sinusoidal–wavy mini-channel heat sink to enhance the cooling process. They found that the thermal performance was agumented when reducing wave length and increasing wave amplitude. The adoption of CFD specifically in the design and optimization of heat exchangers was intensively reviewed by Bhutta et al [26] proving its efficiency and accuracy. Ranganayakulu et al [27] employed CFD simulations for the transient testing of offset and wavy fins of compact plate-fin heat

exchangers. The NTU values of five samples were determined by using maximum slope method. The j-Colburn factors obtained from experiment and CFD were compared within 12% maximum deviation.

To the best knowledge of authors, there has been very little research reported on using CFD in transient testing of heat exchangers similar to single-blow method. *In this work*, a combined experimental and CFD approach was proposed to perform transient testing on three MCRHXs. The CFD model was realistically based on transient conjugated heat transfer of 3D sector of the MCRHX. Therefore, non-adiabatic walls, radial and axial conduction losses were included in the model. Meanwhile, the measured inlet temperature profile was meant to be arbitrary depending on the heater thermal response rather than applying a step change in feed temperature and was entered to the CFD model. Direct curve matching of outlet temperature histories between CFD and experiment were performed. Nusselt number and friction factor correlations for each configuration were obtained.

2- Experimental apparatus and procedure

A test facility was purposely designed for transient testing of annular type heat exchangers based on unidirectional flow condition as represented schematically in Fig.1. It consists of an open airflow circuit, test section and instrumentations. The test facility is supplied with a compressed air at a certain pressure level from a compressor-vessel system.

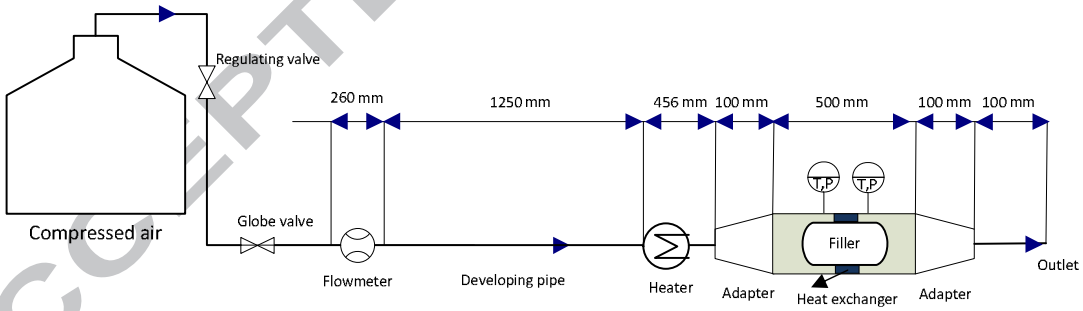

Fig1: schematic of experimental test facility.

The air is allowed to flow in a 2-in pipe and then heated via a 2000 W inline heater (*Omega AHF-14240*), shown in Fig.2(a), before entering the test section. The mean air velocity is measured at the outlet with an anemometer (*TECPEL 712*), shown in Fig.2(b), calibrated with a gas flow meter (*Omega FLMG-10050AL*). The heating power of the heater can be controlled using a Variac transformer (*Carroll & Meynell LTD.*), shown in Fig.2(c). The test section is comprised of two conical adaptors (2in to 5in) (Fig.2(d)), two housing cylinders

with an inner step of 1mm to hold the MCRHX in the middle of the two cylinders (Fig.2(e)), and the MCRHX and the filler assembly (Fig.2(f)). The filler is made of stainless steel with ellipsoidal shape that is hollow from inside with 6 mm thickness and it functions as a flow guide to the MCRHX. All MCRHXs are made of stainless steel and the thermophysical properties are summarized in Table 1. More information on the developed MCRHX configurations can be found in **[28]**.

(a) (b) (c)

(d) (e) (f)

(g)

(h)

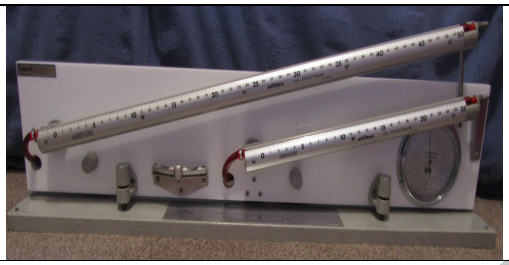

(i)

Fig.2: Test section components, (a) Heater, (b) Anemometer, (c) Variac transformer, (d) Conical converter, (e) Housing cylinder, (f) MCRHX and filler assembly, (g) Assembled test section, (h) Data logger and (i) Inclined micromanometer.

Table 1
Regenerator material thermal properties (SS304L)

Property	Value
Density (kg/m^3)	7850
Specific heat capacity (J/kg. K)	475
Thermal conductivity (W/m. K)	16

Temperature probes (type T) of 3 mm diameter and 0.1 °C accuracy, were used to measure temperatures; at the inlet and outlet of the heater, at four positions (90° offset) at the inlet and the outlet of each MCRHX, as shown in Fig. 3. The transient response of temperature signals is sampled using two data takers (*Pico TC08*) (Fig.2(h)) at a sample rate of 2 Hz connected to a PC. The pressure drop is measured across the test section using (*D and D/2*) pressure tapings connected to a micromanometer (Fig.2(i)) with a minimum scale division of 0.1 mbar and a full scale 50 mbar.

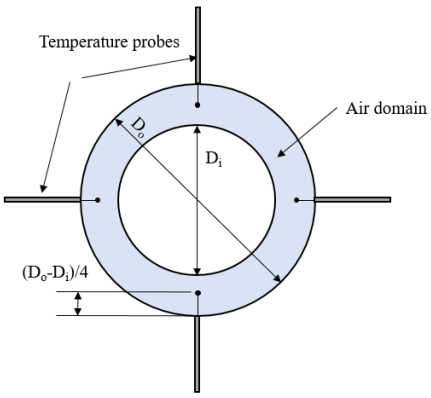

Fig.3: Positions of thermocouples at inlet and outlet of MCRHX.

Once the desired heat exchanger configuration was fitted in the test section, the flow rate was set at the desired amount. For isothermal and Non-isothermal flow experiments, the flow rate was varied in the range from 10 to

50 SCFM and the readings of pressure drop were recorded at isothermal condition. For the Non-isothermal experiments, the heater then was switched on and each test run was allowed for a period of time (normally 1 hour). At that stage, readings of all temperatures were recorded. The maximum outlet temperature of the heater was maintained around 100 °C at each specific flow rate.

3- Theoretical model (CFD)

Since the MCRHX is composed of mini-channels of circular shape, internal fluid flow and heat transfer are the major physics. In experiment, the hot air passes through the channels transporting energy to the MCRHX. Temperature responses of the air are measured at inlet and outlet of the MCRHX. Due to the complexity to insert thermocouples in the miniature channels to measure the solid wall temperature inside the channels, similar approach to single-blow transient method was proposed in this work. The current technique is robust and cost effective compared to single-blow method and steady-state heat transfer measurements. In the conventional single-blow method, the analytical solution of this method imposed an ideal step change in inlet fluid temperature to a constant value to be met in experiment until the new equilibrated temperature is reached. This requires a special controlled compact heater, or using two-fluid streams with a fast response valve, or any mechanism to switch between the two streams, which adds more time and complexity and hence cost to the experimental set-up. In the current set-up, a low heat capacity heater was used to heat up the test core gradually without a step change from a room temperature for a period of time so that the inlet and outlet temperature profiles are measured and sampled for analysis. The heat transfer characteristics can be evaluated by the transient response of the air outlet temperature. Transient conjugated heat transfer simulations were performed on 3D sector of the MCRHX using Comsol multiphysics 5.2a. The inlet thermal response obtained from experiment was entered to the CFD model as inlet boundary condition using piecewise cubic interpolation function. The outlet thermal response predicted is iteratively matched as a whole curve with experiment for each test run. Once the thermal responses are matched within a minimum acceptable deviation, heat transfer coefficient can be calculated from CFD. Table 2 summarizes the main differences between the current approach and the single-blow method.

Table 2
Comparison between current testing technique and single-blow method.

Condition	Transient testing technique	
	Current technique	Single-blow method
Inlet temperature	Arbitrary change	Step change
Fluid properties	Temperature dependent	constant
Steady-state	Not required	required
Thermal losses	Included (non-adiabatic walls, radial and axial conduction)	Non-adiabatic walls and axial conduction can be included
Numerical model	CFD (Conjugate heat transfer)	Analytical (Schumann-Hausen model)
Evaluation technique	Direct curve matching	Depends on NTU value but maximum slope method is recommended.

The computational model is based on the following assumptions:

- The gas is weakly compressible that is its density is only constant with pressure and all other fluid properties are strongly dependent on the temperature field.
- The inlet velocity and the inlet temperature profiles are uniform.
- The effective thermal conductivity of solid matrix $(1-\varepsilon)k_s$) is accounted in simulations.

The governing equations are;

$$\frac{\partial \rho}{\partial t} + \rho \nabla . (\boldsymbol{u}) = 0 \tag{1}$$

$$\rho \frac{\partial u}{\partial t} + \rho (\boldsymbol{u} . \nabla)\boldsymbol{u} = \nabla . [-p\boldsymbol{I} + \mu \ (\nabla \boldsymbol{u} + (\nabla \boldsymbol{u})^T)] \tag{2}$$

$$For\ fluid \qquad \rho C_p (\frac{\partial T}{\partial t} + \boldsymbol{u} . \nabla T) + \nabla . k \nabla T = Q \tag{3}$$

$$For\ solid \qquad (1+\zeta)\rho_s C_{ps} \frac{\partial T}{\partial t} = \nabla . (1-\varepsilon) k_s \nabla T \tag{4}$$

The computational domain is a 3D sector of the heat exchanger as illustrated in Fig.4. Inlet boundary condition is imposed at the inlet with constant velocity in x-direction and the temperature profile collected from experiment.

$$T = T_{inlet}, u = U_m, v = 0, w = 0 \quad (5)$$

The outlet boundary condition is set across the gas outlet as such that convection heat transfer is dominant. The temperature gradient in the normal direction is zero thus,

$$-\mathbf{n}.\mathbf{q}'' = 0 \quad (6)$$

The outlet pressure is set to zero (gauge pressure) and backflow is suppressed. The walls between the fluid and the solid are set as no slip. The symmetry boundary condition is imposed on the two faces of the sector lie in Y-X planes to account for similar physics. Thermally resistive layers are added on the faces lie in X-Z planes to account for the conduction resistance occurs through housing cylinder inner and filler outer walls. A thermal insulation layer (0.04 W/m·K conductance) boundary condition of 12mm thickness was applied on the outer walls of the housing cylinders. The time step was fixed for all simulations to be 1 second as the normal sampling rate. The mesh sequence was based on sweeping the meshed inlet faces (free triangular elements) over the total length of the sector so that the resultant elements are composed of prism and hexahedral elements. The mesh sensitivity analysis showed that when the mesh was further refined below 156, 636 of total elements, simulation results only changed by less than 1%.

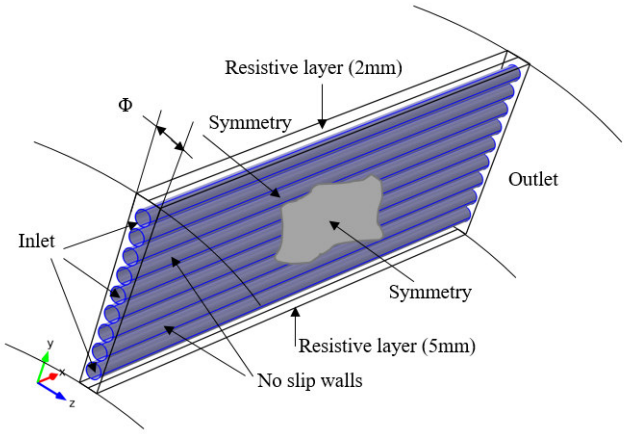

Fig.4: Computational domain of 3D sector of the heat exchanger.

It should be emphasized that the results of the CFD model were scaled by introducing the factor (ζ) into Eq.4 to overweigh any boundary condition that can't be feasibly included in the considered computational domain [29]. In the current CFD model, the computational domain considered is only a 3D sector of the heat exchanger (test core) including the inner and outer walls of the housing cylinders and the filler attached to the heat exchanger with a length equals the heat exchanger length as shown in Fig.4. However, these walls attached to MCRHX (designated as resistive layers in the figure) extend 3 times and 8 times the heat exchanger length, as shown in Fig.2(f), for the filler walls and housing walls, respectively. Therefore, heat capacity of these walls and the heat loss by axial conduction starting from the outlet of the heater which are not captured in the current computational domain, were overweighed. This constant is varied by trial and error and their values at different flow conditions are summarized in Table 3. The absolute value of the total residual between measurement and prediction data points are minimized by using least square criterion [13].

$$R = \left[\sum_{n=1}^{3600} (T_{cal} - T_{exp})^2\right]^{0.5} \tag{7}$$

Table 3
(ζ) values under different flow conditions.

MCRHX type					
1.5mm		1mm		0.5mm	
Re	ζ	Re	ζ	Re	ζ
146	5.35	146	6	58	4.75
229	5.75	229	4.75	97	4.25
374	4.75	373	4.28	152	3.8
507	4.5	475	4.5	196	4

684	4.3	641	4	242	3.25

The total heat flux entered to the MCRHX, $\mathbf{q''_{-tot}}$, can be calculated in terms of the air temperature difference measured at the inlet and outlet, the specific heat capacity, mass flow rate and internal surface area of the MCRHX,

$$\mathbf{q''_{-tot}} = \dot{m} C_p \Delta T / A_s \tag{8}$$

The net heat flux transferred to the MCRHX, $\mathbf{q''_{-net}}$, is calculated from CFD by

$$\mathbf{q''_{-net}} = k_f \left[\left(\frac{\partial T}{\partial r} \right)_{wall} \right]_x \tag{9}$$

The results of the total heat flux and the net heat flux transferred to the MCRHX at different flow rates, were represented in Fig.5. It is clear that heat flux shows an increasing trend with flow rate due to the forced convection. As depicted, the difference between total and net heat flux represents the heat loss from the test core (MCRHX). This implies the importance of the factor (ζ) which adds an artificial heat capacity of the walls attached to the test core that extends beyond the considered computational domain as previously explained and hence the transient axial conduction loss through these walls starting from the heater outlet up to the outlet of the MCRHX, is accounted for accordingly. In the base case, this factor approaches zero value if the heater is located just upstream the MCRHX. The highest heat loss of 142 W was observed for 1mm MCRHX at the maximum flow rate of 50 SCFM compared to 41 W and 74 W for 0.5mm and 1.5mm MCRHX's, respectively.

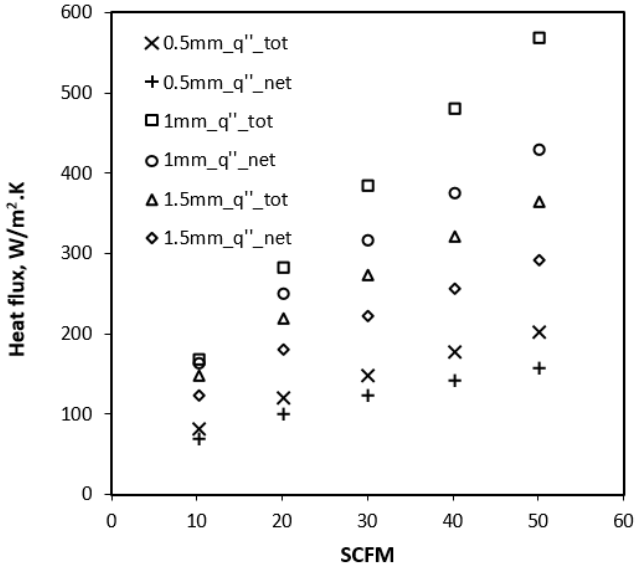

Fig.5: Total and net heat flux transferred to the three MCRHX's at different flow rates.

The temperature histories of inlet and outlet from experiment and CFD can be expressed in a nondimensionalized form for comparison as

$$\theta = \frac{T - T_{ref}}{T_f - T_{ref}} \tag{10}$$

Since the maximum slope method is not used in this work, the nondimensionalized time variable can be conveniently expressed as

$$\tau = \frac{t}{t_f} \tag{11}$$

4- CFD metrics

Prior to the procedure of transient simulations of the MCRHX, the testing metrics of CFD computations is a prerequisite to evaluate its accuracy. Since the flow is developing inside the MCRHX, a replication of macroscopic level of hydrodynamically and thermally developing laminar flow of a single channel was initially conducted using steady state simulation. A 3D circular tube sector of (1 in) diameter and (12 in) length was selected as the computational domain to calculate fluid flow and heat transfer characteristics under constant wall temperature condition of 310 K. Uniform inlet velocity boundary (at Re=100) and pressures outlet of 1 atm with

no backflow were applied at the inlet and outlet of the channel, respectively. Mesh sensitivity analysis was initialized with varying the mesh sequence (free tetrahedral) from coarse to extra fine size. It was found that the change of Nusselt number is less than 1.3% when finer mesh (with total number of elements = 283,920) was compared to the extra-fine sequence. The velocity and temperature contours are plotted in Fig. 6(a)-(b). It is clearly shown that both hydrodynamic and thermal boundary layers are developing downstream of the tube inlet.

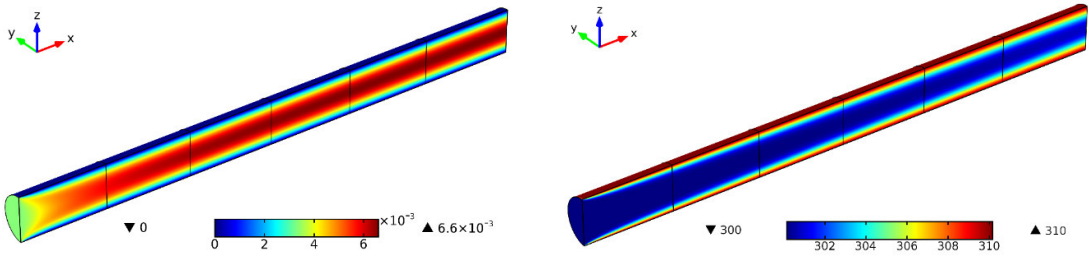

(a) (b)

Fig.6: (a) velocity contours (m/s), (b) temperature contours (K), along the tube.

A first check to carry out was to calculate the ratio of the maximum velocity magnitude to the average velocity magnitude at the end of the tube and the product of Reynolds number with friction factor. The comparison made in Table 4 has shown good agreement with the available analytical solution [30].

Table 4
Comparison between CFD results and analytical data for fully developed tube flow.

Parameter	CFD	Analytical solution
$\mathbf{u_{max}/u_{mean}}$	1.97	2
fRe	17.4	16

In order to validate the CFD results of the obtained Nu number in the case of developing flow, Hausen's correlation [31] was selected for the comparison which is recommended for a combined entry length under constant wall boundary condition.

$$\overline{Nu_D} = 3.66 + \left[\frac{0.0668 G_{Z_D}}{1 + 0.04 {G_{Z_D}}^{\frac{2}{3}}}\right] \tag{12}$$

Where G_{Z_D} is a dimensionless parameter defined as

$$G_{Z_D} = \left(\frac{D_h}{x}\right).Re.Pr \tag{13}$$

As can be seen in Fig.7, the results of the average Nusselt number compares reasonably well with Hausen's correlation within a deviation in the range of 5-11%, giving assurance and confidence in the present CFD methodology.

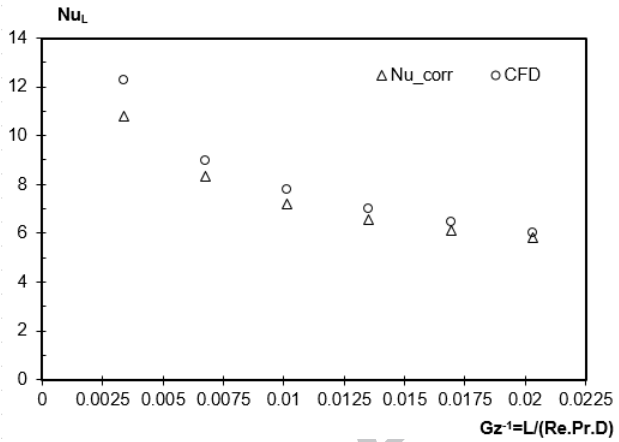

Fig.7: Nusselt number for laminar developing pipe flow.

5- Data analysis and Uncertainty.

Friction factors. The friction factor for each MCRHX is calculated from the predicted pressure drop and the mean air velocity,

$$f = \left(\frac{\Delta P_{cal}}{\frac{1}{2}\rho {U_m}^2}\right)\frac{D_h}{L} \tag{14}$$

Since the maximum deviation between predicted pressure drop, ΔP_{cal} and experimental pressure drop, ΔP_{exp} is 8% and the individual uncertainties for ΔP_{exp} and U_m are 0.2% and 1.4%, respectively. Therefore, the maximum uncertainty in calculating f is less than 9% based on reference [32].

Heat transfer coefficient. Heat transfer coefficient is calculated from CFD after matching the air temperature responses at the outlet of the MCRHX with experiment. From the knowledge of net heat flux, average bulk temperature and the average wall temperature, the average heat transfer coefficient can be calculated from,

$$h = \frac{q''_{-net}}{T_b - T_w} \tag{15}$$

The errors in estimating heat transfer coefficients are mainly due to uncertainty in temperature measurement and the deviation in temperatures between measured and predicted values (the root-mean-square difference). The uncertainty in temperature measurement by temperature probes and data taker resolution is 1%. The maximum deviation in temperatures recorded between predicted and measured values is less than 9%. Therefore, the maximum uncertainty in calculating h is less than 10%.

6- Results and discussion

A sample of the temperature contours of the three MCRHXs at 10 SCFM and test run time of (3600s) were presented in Fig. 8. As can be seen, the isothermal contours of the solid temperature are not uniform along the whole length of MCRHX in flow direction (x-axis). The profile gradually becomes a curved-shape near the outlet due to heat lost to the attached walls and the axial conduction losses.

The typical plots of air inlet and outlet temperatures histories for the three MCRHXs are presented in Fig.9 to Fig.11. The inlet measured temperature history was entered to the CFD model and hence the predicted and measured outlet temperature histories were compared (square solid points represent measured values and the dashed line represents predicted values). In general, the predicted values are in good agreement with the measured ones. This has given confidence in the developed test facility and the proposed computational approach. The heating period was maintained for 1hour for all tests. It should be noted that due to the restriction that the heater has a fixed heating power and the outlet temperature of the heater is merely dependent on the flow rate, the maximum temperature was set to roughly 100°C for all test runs.

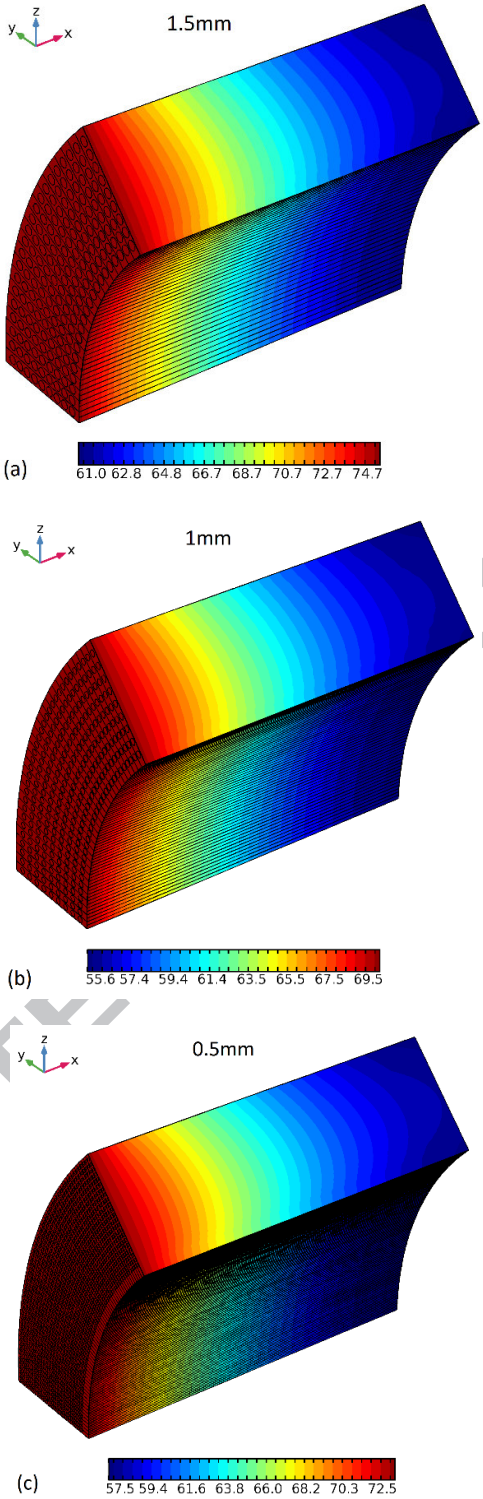

Fig.8: Sample of temperature contours (in °C) of the three MCRHXs at 10 SCFM and t = 3600s.

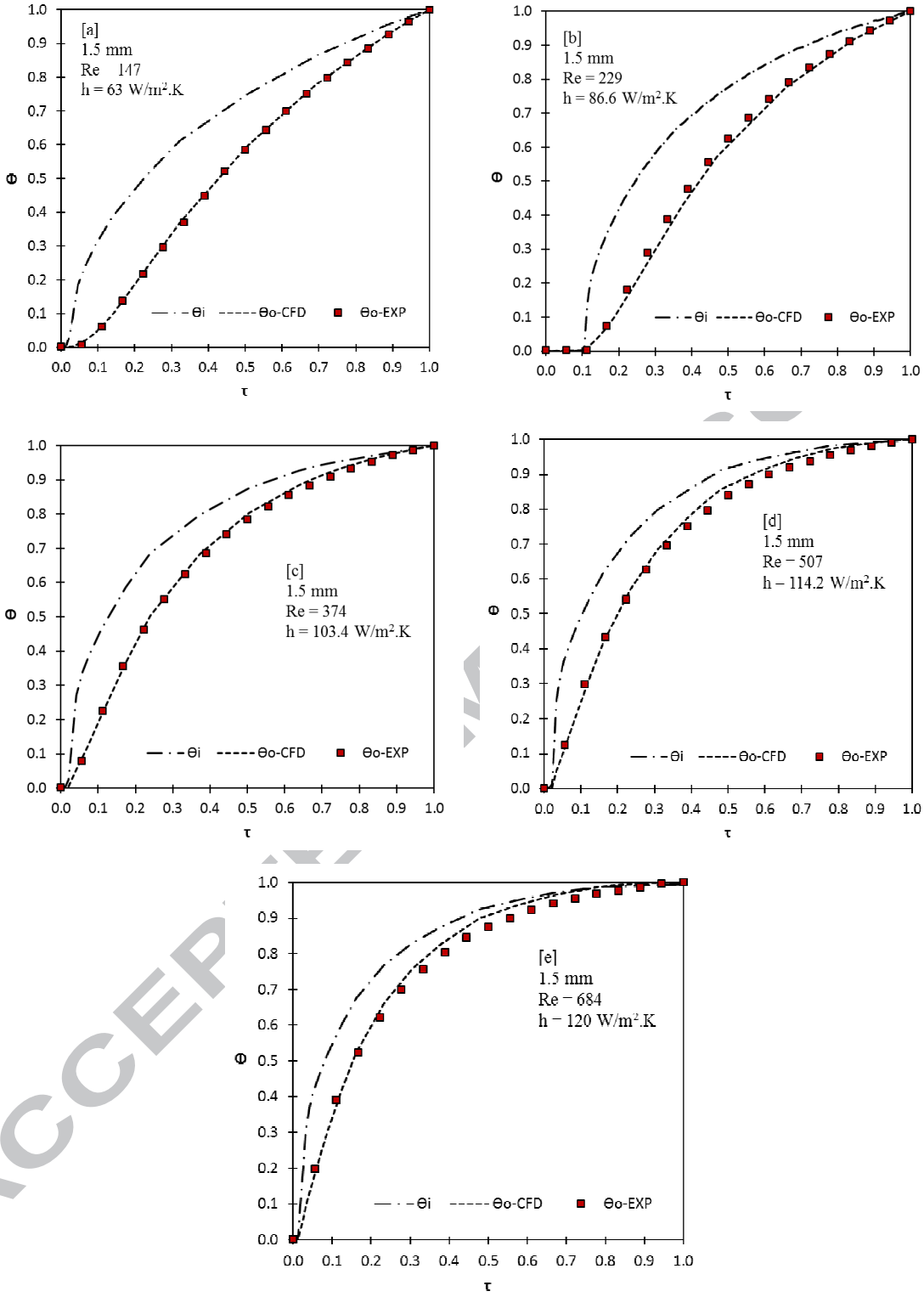

Fig.9: Comparison of inlet and outlet temperatures histories for 1.5mm MCRHX.

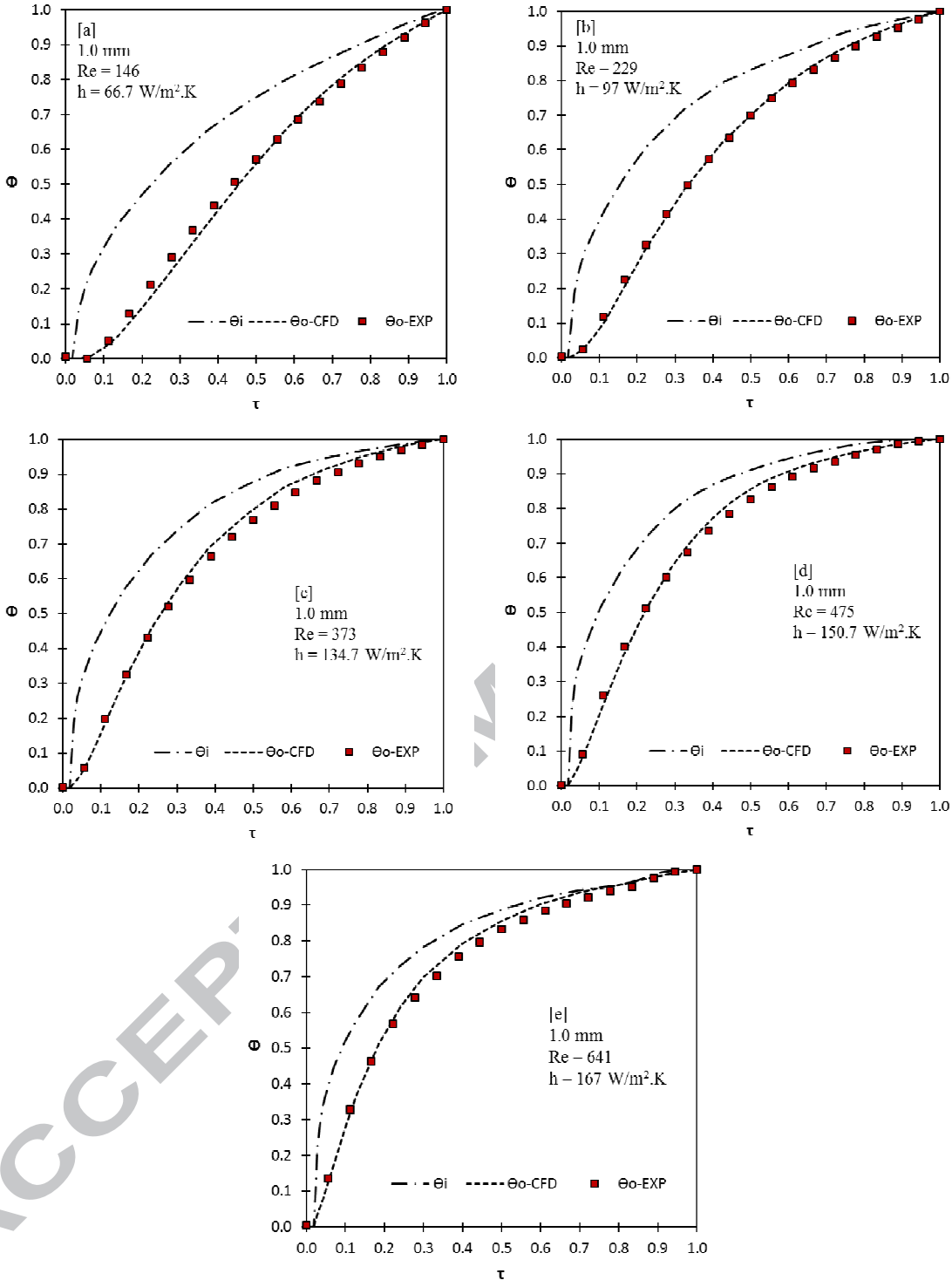

Fig.10: Comparison of inlet and outlet temperatures histories for 1mm MCRHX.

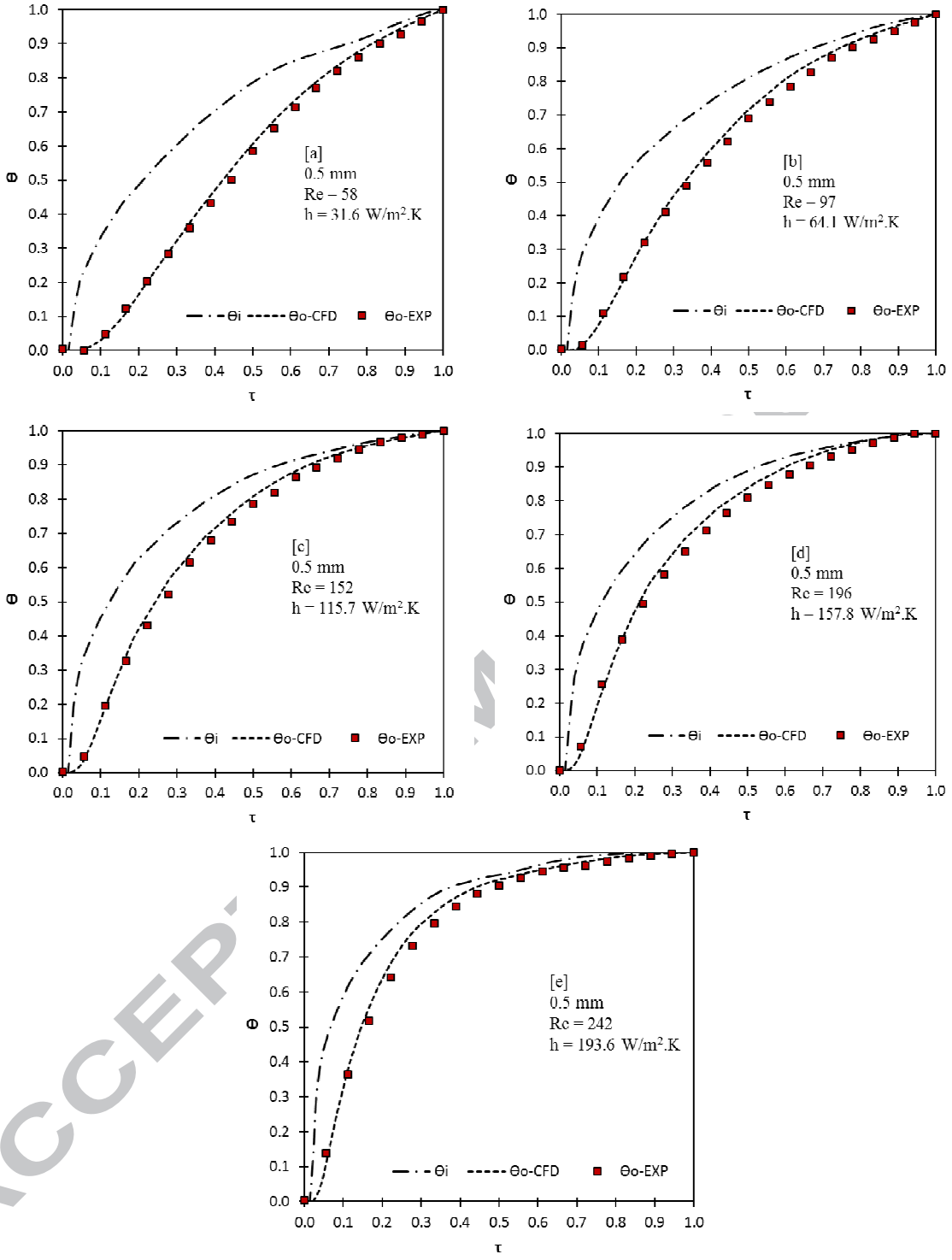

Fig.11: Comparison of inlet and outlet temperatures histories for 0.5mm MCRHX.

As shown in Figs.9(a)-(e), as inlet velocity increases, the incremental rate in temperature, Θ increases. For example, at a time ratio of 0.3 and different Re number, 147 and 684, respectively, the temperature incremental rate reads 0.325 and 0.724. This result is natural and it agrees with the principles of forced convection and it was observed for all configurations. The (ζ) values were varied by trial and error until the corresponding thermal responses at outlet are matched between CFD and measurements. At each test case, the heat transfer coefficient was calculated from CFD and was shown on the legends. For 1.5mm MCRHX, as depicted in the heat transfer coefficient varies from 63 to 120 W/m^2.K at Reynolds number from 147 to 684. For 1mm MCRHX, as depicted in Fig.10(a)-(e), the heat transfer coefficient varies from 66.7 to 167 W/m^2.K at Reynolds number from 146 to 641. Similarly, the heat transfer coefficient varies from 31.6 to 193.6 W/m^2.K at Reynolds number from 58 to 242 for 0.5mm MCRHX, as depicted in Fig.11(a)-(e). In terms of heat transfer coefficient, larger diameter channels experience relatively low heat transfer coefficients at higher Reynolds number (over 240) due to the limited heat transfer surface area. In order to quantify the interstitial heat transfer coefficient (q_sf), the specific solid surface area is used for each configuration which is defined as the ratio of the matrix surface area exposed to the gas to the volume of the matrix and can be calculated in terms of volumetric porosity (ε) and hydraulic diameter (D_h). The calculated specific areas for 0.5mm, 1mm and 1.5mm configurations are 2617 (1/m), 1565 (1/m) and 1156 (1/m), respectively. The interstitial heat transfer coefficients vs. Reynolds number are shown in Fig.12 for the three MCRHXs.

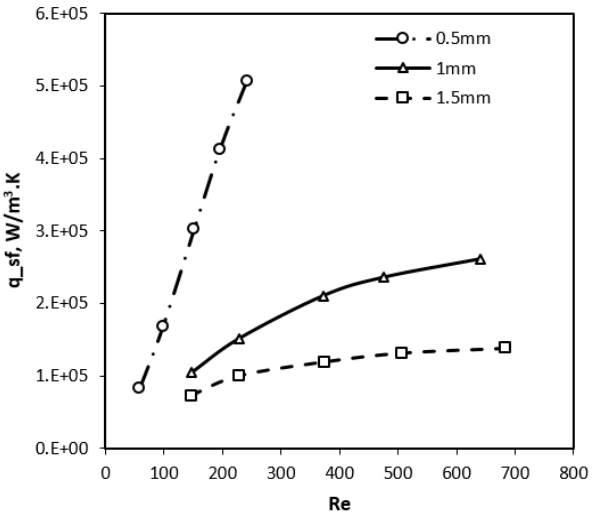

Fig.12: interstitial heat transfer coefficients vs. Reynolds number for the three heat exchangers.

As can be seen that the specific surface area exposed to the working gas plays an important role in maximizing the thermal performance of the heat exchanger. Since heat transfer resistance between the gas and the solid is much higher than the resistance inside the MCRHX. Therefore, higher values of interstitial heat transfer coefficients were obtained for 0.5mm configuration compared to 1mm and 1.5mm ones due to the increased specific surface area.

Fig.13 shows that the average Nusselt number increases with Reynolds number. For larger diameter channels, higher values of Nusselt number is depicted due to the higher values of hydraulic diameters. However, the small hydraulic diameter indicates faster thermal response at a small range of Reynolds number (60 to 250) compared to larger diameter channels (150 to 700). For smaller channels (0.5mm), it is clear that Nusselt number almost varies linearly with Reynolds number with a slope higher than that of larger diameter ones. It is noteworthy that at Reynolds number higher than 300, the Nusselt number values of small diameter MCRHX will be superior to large ones.

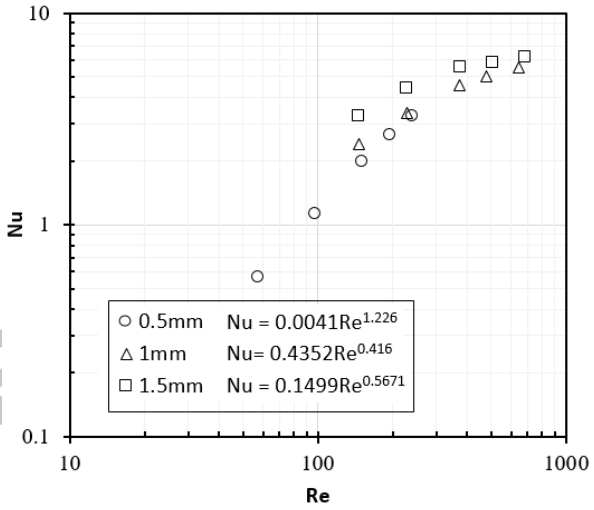

Fig.13: Average Nusselt number vs. Reynolds number for the three heat exchangers.

The fluid flow characteristics, in terms of pressure drop, were obtained from CFD simulations for each configuration and compared to experiment as shown in Fig.14. As can be seen that data of pressure loss compares well with experiment with maximum deviation of 9%. The trends are almost linear with fluid inlet velocity for all MCRHX configurations. The inertial loss part is not significant in the channels due to the absence of flow separation and vortices. In general, the highest pressure loss is observed for 0.5mm MCRHX.

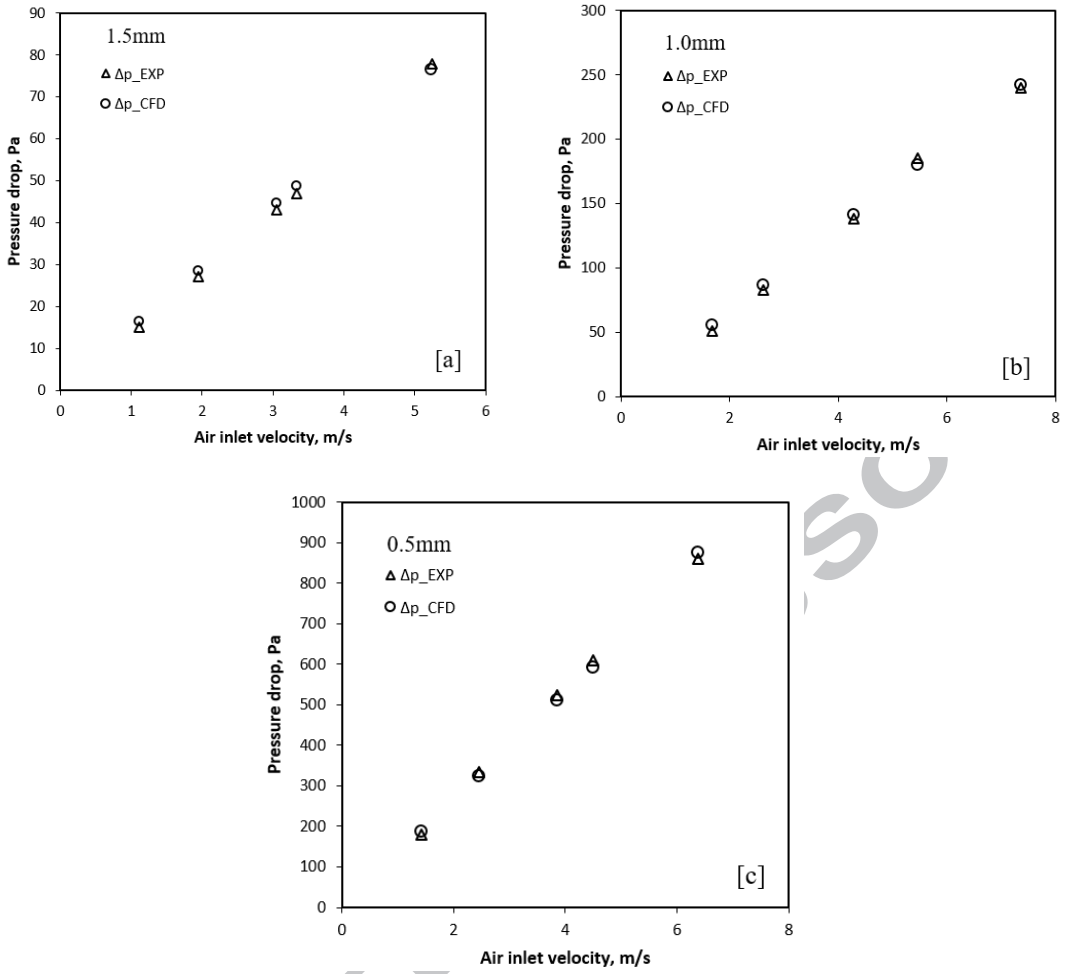

Fig.14: comparison of pressure drop across the three heat exchangers between CFD and experiment, (a) 1.5mm, (b) 1mm, (c) 0.5mm.

The simulation results for friction factors were plotted in Fig.15. The average friction factor shows a decreasing trend with increasing Reynolds number for all configuration. The friction factor correlations are close to Darcy friction factor for laminar flow case. This indicated that the use of classical friction correlation for mini-channels accurately apply in the present investigated range.

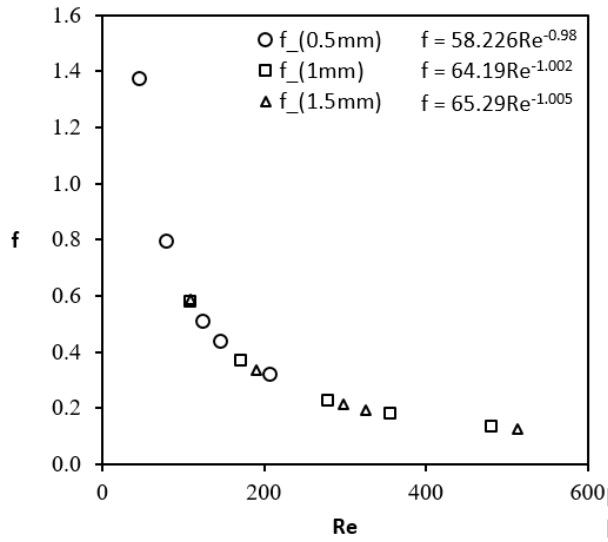

Fig.15: friction factor vs. Reynolds number for the three MCRHXs.

7- Conclusion and recommendations

A combined experimental and CFD study has been performed on three MCRHXs with different channel hydraulic diameter of 1.5, 1 and 0.5mm. Heat transfer and fluid flow characteristics were obtained for each configuration based on transient testing similar to single-blow method. Direct curve matching using least square criterion was used to match temperature outlet histories of CFD and experimental data. The results showed that this combined approach is time effective and reliable since arbitrary inlet thermal response can be used instead of step change in feed temperature during experiments. Moreover, there is no restriction to include different losses in the test core, such as radial and axial conduction, for better accuracy. Further study is recommended for single channels with the same investigated range of hydraulic diameters to compare with the classical correlatios at uniform heat flux or temperature conditions.

Acknowledgments

The authors acknowledge the Ph.D. sponsorship received from University of Benghazi and the Libyan Ministry of Higher Education and Scientific Research.

References

1- Kandlikar SG, Grande WJ. Evolution of Microchannel Flow Passages--Thermohydraulic Performance and Fabrication Technology. Heat transfer engineering. 2003;24(1):3-17.

2- Hausen H. Theory of heat exchange in regenerators, Zeitschrift fur Angewandte Mathematik und Mechanik 1929;9(3):173-200.

3- Schumann TE. Heat transfer: a liquid flowing through a porous prism. Journal of the Franklin Institute. 1929;208(3):405-416.

4- Locke GL. Heat transfer and flow friction characteristics of porous solids. Stanford University. Department of Mechanical Engineering; 1950.

5- Loehrke RI. Evaluating the results of the single-blow transient heat exchanger test. Experimental Thermal and Fluid Science. 1990;3(6):574-580.

6- Cai ZH, Li ML, Wu YW, Ren HS. A modified selected point matching technique for testing compact heat exchanger surfaces. International journal of heat and mass transfer. 1984;27(7):971-978.

7- Liang CY, Yang WJ. Modified single-blow technique for performance evaluation on heat transfer surfaces. ASME J. Heat Transfer. 1975;97(1):16-21.

8- Mullisen SR, Loehrke RI. A transient heat exchanger evaluation test for arbitrary fluid inlet temperature variation and longitudinal core conduction. ASME J. Heat Transf. 1986; 108: 370–376.

9- Chen PH, Chang ZC. Measurements of thermal performance of cryocooler regenerators using an improved single-blow method. International journal of heat and mass transfer. 1997;40(10):2341-2349.

10- Chen PH, Chang ZC, Huang BJ. Effect of oversize in wire-screen matrix to the matrix-holding tube on regenerator thermal performance. Cryogenics. 1996;36(5):365-372.

11- Pucci PF, Howard CP, Piersall CH. The single-blow transient testing technique for compact heat exchanger surfaces. Journal of Engineering for Power. 1967;89(1):29-38.

12- Chang ZC, Hung MS, Ding PP, Chen PH. Experimental evaluation of thermal performance of Gifford–McMahon regenerator using an improved single-blow model with radial conduction. International journal of heat and mass transfer. 1999;42(3):405-413.

13- Heggs PJ, Burns D. Single-blow experimental prediction of heat transfer coefficients: A comparison of four commonly used techniques. Experimental Thermal and Fluid Science. 1988;1(3):243-251.

14- Krishnakumar K, John AK, Venkatarathnam G. A review on transient test techniques for obtaining heat transfer design data of compact heat exchanger surfaces. Experimental Thermal and Fluid Science. 2011; 35(4):738-43.

15- Baclic BS, Gvozdenac DD, Sekulic DP, Becic EJ. Laminar heat transfer characteristics of a plate-louver fin surface obtained by the differential fluid enthalpy method. Adv. Heat Exch. Des. 1986:21-27.

16- Younis LB, Viskanta R. Experimental determination of the volumetric heat transfer coefficient between stream of air and ceramic foam. International Journal of Heat and Mass Transfer. 1993;36(6):1425-34.

17- Luo X, Roetzel W, Lüdersen U. The single-blow transient testing technique considering longitudinal core conduction and fluid dispersion. International Journal of Heat and Mass Transfer. 2001;44(1):121-129.

18- Shaji K, Das SK. The effect of flow maldistribution on the evaluation of axial dispersion and thermal performance during the single-blow testing of plate heat exchangers. International Journal of Heat and Mass Transfer. 2010;53(7):1591-1602.

19- Kandlikar SG, Grande WJ. Evolution of Microchannel Flow Passages--Thermohydraulic Performance and Fabrication Technology. Heat transfer engineering. 2003;24(1):3-17.

20- Asadi M, Xie G, Sunden B. A review of heat transfer and pressure drop characteristics of single and two-phase microchannels. International Journal of Heat and Mass Transfer. 2014;79:34-53.

21- Dixit T, Ghosh I. Review of micro-and mini-channel heat sinks and heat exchangers for single phase fluids. Renewable and Sustainable Energy Reviews. 2015;41:1298-1311.

22- Reay D, Ramshaw C, Harvey A. Process Intensification: Engineering for efficiency, sustainability and flexibility. Butterworth-Heinemann; 2013.

23- Caney N, Marty P, Bigot J. Friction losses and heat transfer of single-phase flow in a mini-channel. Applied thermal engineering. 2007;27(10):1715-1721.

24- Liu X, Yu J. Numerical study on performances of mini-channel heat sinks with non-uniform inlets. Applied Thermal Engineering. 2016;93:856-864.

25- Khoshvaght-Aliabadi M, Sahamiyan M, Hesampour M, Sartipzadeh O. Experimental study on cooling performance of sinusoidal–wavy minichannel heat sink. Applied Thermal Engineering. 2016;92:50-61.

26- Bhutta MM, Hayat N, Bashir MH, Khan AR, Ahmad KN, Khan S. CFD applications in various heat exchangers design: A review. Applied Thermal Engineering. 2012;32:1-12.

27- Ranganayakulu C, Luo X, Kabelac S. The single-blow transient testing technique for offset and wavy fins of compact plate-fin heat exchangers. Applied Thermal Engineering. 2017;111:1588-1595.

28- Alfarawi S, AL-Dadah R, Mahmoud S. Potentiality of new miniature-channels Stirling regenerator. Energy Conversion and Management. 2017;133:264-74.

29- Hwang JJ, Hwang GJ, Yeh RH, Chao CH. Measurement of interstitial convective heat transfer and frictional drag for flow across metal foams. Journal of heat transfer. 2002;124(1):120-129.

30- Kakaç S, Shah RK, Aung W, editors. Handbook of single-phase convective heat transfer. New York et al.: Wiley; 1987.

31- Hausen H. Darstellung des Warmeuberganges in Rohren durch verallgemeinerte Potenzbeziehungen. Z. VDI Beih. Verfahrenstech. 1943;4:91-98.

32- Moffat RJ. Describing the uncertainties in experimental results. Experimental thermal and fluid science. 1988;1(1):3-17.

Highlights

- Combined experimental and CFD approach was proposed to substitute single-blow technique.
- Mini-channel regenerative heat exchangers (MCRHX) were investigated.
- Direct curve matching technique was utilized.
- Heat transfer is enhanced by reducing the channels hydraulic diameter.
- Nusselt number and friction factor correlations were developed.